ECS Transactions, 66 (7) 51-56 (2015)
10.1149/06607.0051ecst ©The Electrochemical Society

The Effect of Interfacial Contamination on Antiphase Domain Boundary Formation in GaAs on Si(100)

C. S. C. Barrett[a], A. G. Lind[a], X. Bao[b], Z. Ye[b], K. Y. Ban[b] , P. Martin[b], E. Sanchez[b], and K. S. Jones[a]

[a] Department of Materials Science and Engineering, University of Florida, Gainesville, Florida 32611, USA
[b] Applied Materials, 974 East Arques Avenue, Sunnyvale, California 94085, USA

The suppression of defects such as antiphase domain boundaries (APBs) is a key challenge in the effort to integrate III-V compound semiconductor devices on Si. The formation of APBs naturally arises from growing a polar material on a nonpolar substrate. Surface contamination present on the substrate prior to growth can also disrupt the ordering of atoms in an epitaxial layer and lead to extended defects. In this study, the amount of contamination on Si(100) wafers was varied by approximately an order of magnitude to investigate the effect on formation of APBs in an epitaxial GaAs film grown by MOCVD. The results indicate a direct correlation between the interfacial oxygen and carbon impurity dose and the APB density.

Introduction

The drive for increased performance in electrical devices at small scales has prompted renewed interest in the use of III-V compound semiconductors. Some III-V materials, such as InAs, offer electron mobilities that are more than 10 times that of Si (1). The direct growth of high-quality III-V layers on Si wafers will help to reduce the economic impact of implementing future device technologies. Industry tools are based on large Si wafers which help to increase throughput and are relatively inexpensive. The use of metal-organic chemical vapor deposition (MOCVD) systems also helps to improve throughput versus other III-V on Si epitaxy approaches such as molecular beam epitaxy (MBE). Unfortunately, there are several challenges in the growth of III-Vs on Si including reduction of defects arising from lattice mismatch and polar-on-nonpolar growth. For example, InAs has a lattice constant that is about 12% greater than that of Si (6.06 Å vs. 5.43 Å). This mismatch leads to a high density of dislocations which can propagate through the layer and degrade electrical performance (2). Various methods have been studied for decreasing the threading dislocation density in III-V layers on Si, such as aspect ratio trapping (ART) and the use of buffer layers with intermediate lattice constants (1). GaAs has been commonly used as a buffer layer due to its intermediate lattice constant (5.65 Å) and relatively large bandgap (~1.4 eV) for electrical isolation. These methods, however, do not directly address the polarity issue.

The growth of a polar III-V material on a nonpolar Si substrate can lead to the formation of antiphase domain boundaries (APBs). These defects arise from single-steps on the Si surface that disrupt ordering of atoms in the epitaxial III-V layer. Similar atoms become bonded to one another across the boundary, e.g. Ga-Ga and As-As bonds for GaAs. APBs can be eliminated by the formation of a double-stepped Si surface or self-annihilation with another APB (3). Conventional methods for creating double-steps on a Si wafer include off-cutting the wafer (4) or annealing the wafer at elevated temperatures (near 1000 ºC) prior to III-V layer growth (5, 6). However, these treatments are not compatible with industrial processing of Si wafers which requires planar substrates and reduced thermal budgets. Thus, growth conditions must be optimized to induce complete self-annihilation of APBs within the bulk of the III-V layer before they reach the surface. This is especially important for the use of GaAs as a buffer layer so that APBs do not propagate into subsequent layers.

It is well known that surface contamination on the Si substrate can lead to overall degradation of epitaxial III-V film quality (2, 7-10). Oxygen and carbon are the most common sources of contaminants. The presence of impurities on the Si surface can cause the formation of stacking faults and other defects during growth. The effect on the formation of APBs is not as well-studied. It is hypothesized that the surface contaminants also promote APBs because of the disruption in atomic ordering of the growing layer, similar to the effect of single-steps. In this study, the effect of interfacial contamination on the formation of APBs in GaAs films grown on Si(100) by MOCVD with reduced thermal processing is investigated. The interfacial doses of oxygen and carbon are quantified and correlated to the APB densities in the GaAs layers.

Experimental

GaAs on Si Growth

Growth of GaAs was carried out on 300 mm Si(100) wafers (exact cut) by an Applied Materials III-V MOCVD system. Trimethylgallium (TMGa) and tertiarybutylarsine (TBAs) precursors were utilized as sources for Ga and As, respectively. The growth process followed the well-established two-step scheme of a low temperature nucleation layer plus a high temperature bulk layer at typical reduced pressure ambients for improved epitaxial GaAs-on-Si crystal quality (11, 12). The nominal thickness of the films was 450 nm.

Prior to the growth of the GaAs layer, the substrates were cleaned using the Siconi™ method (13). In this process, species generated in a dry remote fluorinated plasma selectively react with and consume SiO_2 on the substrate surface. This method provides an alternative to conventional high temperature treatments for Si substrates that thermally desorb native oxide and contaminants. The pre-growth clean in this study was modulated in order to vary the relative amount of residual impurity at the GaAs/Si interface. All growth conditions were otherwise identical for the samples.

Analytical Methods

In order to determine the APB density in the grown GaAs films, samples were stained in a HF(49%):HNO_3(69%):H_2O (10:1:3 by volume) solution for a short time (<10 s). This solution has been demonstrated to selectively etch APBs versus other defects in epitaxial GaAs layers grown on Si (14-16). After staining the samples, a scanning electron microscope (SEM) was used to take images of the sample surfaces in various areas. The images were analyzed using ImageJ software (17) to calculate an APB density for each sample. The APB density is defined as the APB line length per area, i.e. the total length of APB features in an image over the area represented by the image.

The thickness and morphology of the GaAs layers were analyzed using transmission electron microscopy (TEM). Secondary ion mass spectrometry (SIMS) with a Cs ion beam was used to quantify the interfacial carbon and oxygen doses in the samples.

Results and Discussion

Interfacial Contamination

Concentration-depth profiles were obtained by SIMS for various elements within the grown GaAs layer. Of particular interest were the interfacial peaks of oxygen and carbon. These peaks are indicative of contaminants such as oxide or carbide particles that were present on the Si substrate surface prior to growth. The interfacial peaks for oxygen and carbon of two samples with varied pre-clean conditions are shown in Fig. 1(a) and 1(b), respectively. Note that the peaks are offset because the interface positions were normalized to growth thickness as determined by cross-sectional TEM (XTEM). It is evident that Sample 2 has greater peak concentration of oxygen and carbon at the GaAs/Si interface than Sample 1.

The interfacial doses of oxygen and carbon for Sample 1 and Sample 2 were calculated by integrating the respective interfacial peaks in Fig. 1(a) and 1(b). The "shoulder" region of the carbon interface profiles was not included in the calculation of carbon dose. It was found that Sample 1 exhibited a dose of approximately $7.3x10^{11}$ atoms/cm^2 for oxygen and $1.9x10^{14}$ atoms/cm^2 for carbon. Sample 2 had a dose of $4.0x10^{12}$ atoms/cm^2 for oxygen and $1.7x10^{15}$ atoms/cm^2 for carbon. This difference in both oxygen and carbon contamination provided a good variance in order to study the effect on APB density.

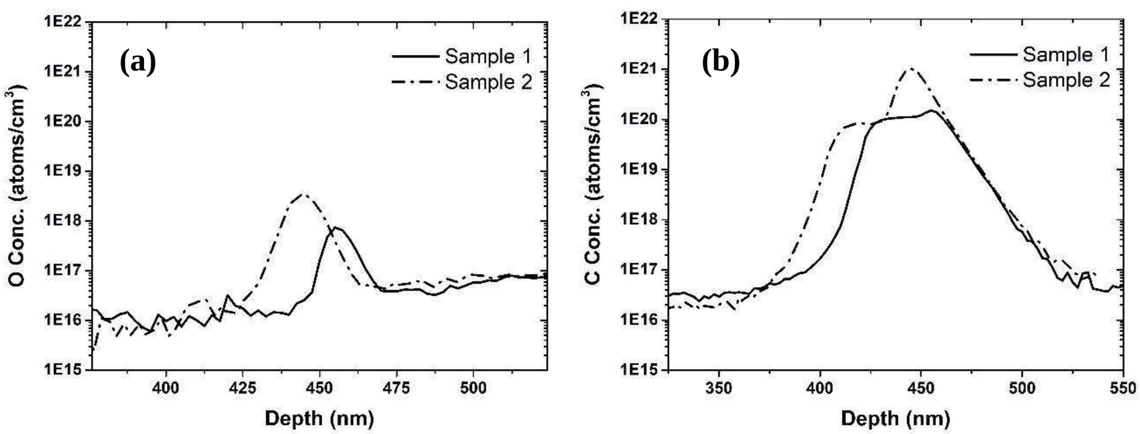

Figure 1. As-grown SIMS profiles of interfacial oxygen (a) and carbon (b) peaks for GaAs on Si samples with varied pre-clean. Sample 2 exhibits greater oxygen and carbon peak concentrations, indicating a larger amount of interfacial contamination. Peaks positions are offset based on layer thickness as determined by XTEM.

APB Density

After growth, the samples were processed using the HF/HNO_3 stain to determine the APB densities. The SEM images for representative areas of Sample 1 and Sample 2 are shown in Fig. 2(a) and 2(b), respectively. It is immediately apparent that there is a significant difference in both the density and behavior of APBs. For Sample 1, the domains are much more contained and exhibit clear faceting behavior. Conversely, Sample 2 possesses APBs that extend for relatively long distances and it is difficult to identify regions of a single domain. By analyzing the line length of APBs per area, it was determined that Sample 1 had an APB density of 0.14±0.01 μm^{-1} and Sample 2 had an APB density of 3.2±0.2 μm^{-1}. The increased APB density in Sample 2 corresponds to the greater interfacial impurity dose (~5-10x that of Sample 1 for oxygen and carbon, respectively).

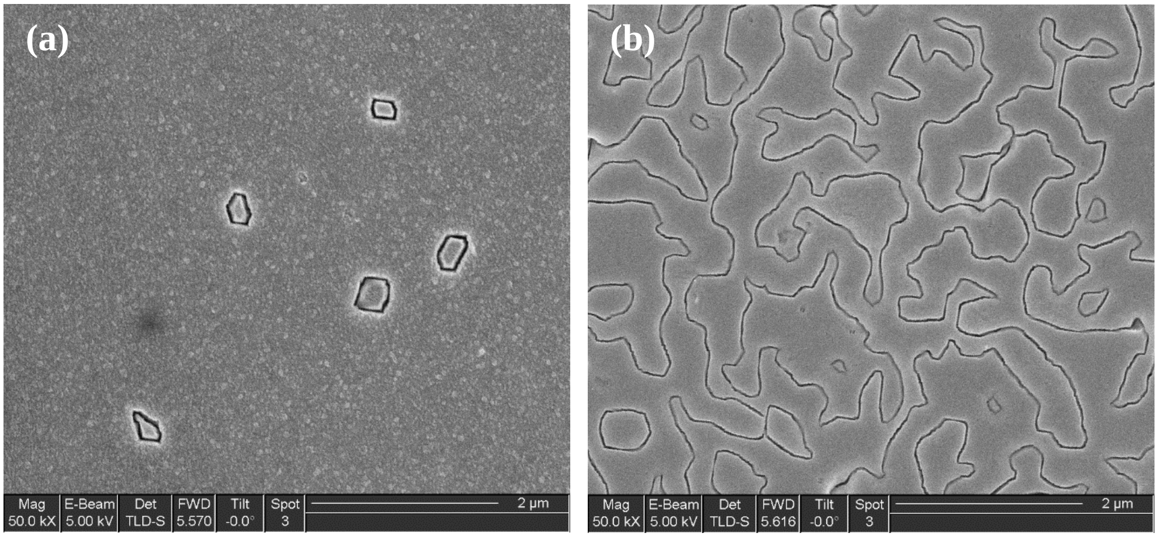

Figure 2. Plan-view SEM images of Sample 1 with lower oxygen and carbon interfacial dose (a) and Sample 2 with higher oxygen and carbon interfacial dose (b) after application of HF/HNO_3 chemical stain. APBs are clearly visible as features of dark contrast. The APB density dramatically increases with an approximately 5-10x increase in oxygen and carbon interfacial dose.

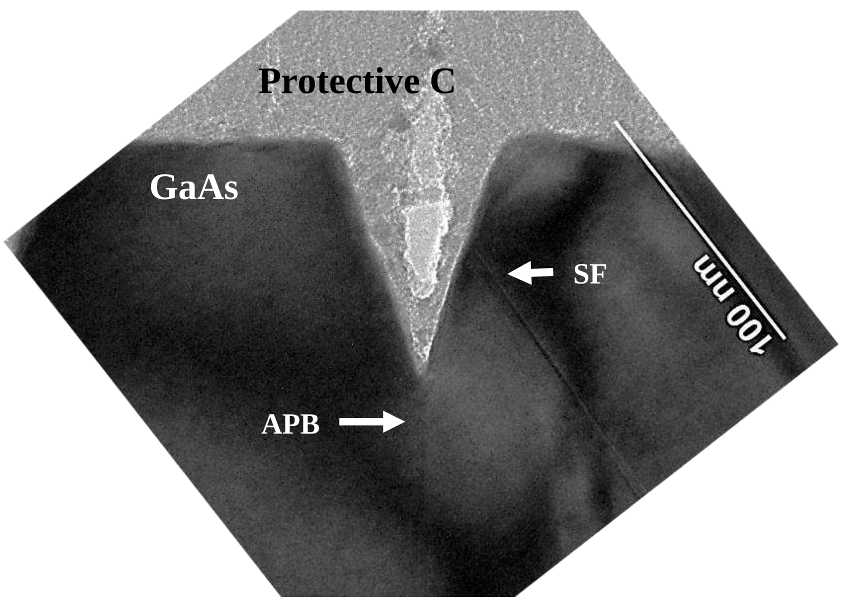

Figure 3. XTEM of etch pit in Sample 2 formed by HF/HNO_3 stain showing selectivity of etching for APB. Other defects, such as a stacking fault (SF) visible in the image, are not as reactive with the solution over the time scale of the etch.

The selectivity of the HF/HNO_3 stain for APBs was confirmed by XTEM analysis of an etched specimen of Sample 2 (Fig. 3). The stain forms an etch pit in the surface of the sample that follows the contrast line of a vertical APB. A stacking fault is observed intersecting with the edge of the etch pit. It is clear that the HF/HNO_3 solution etches down an APB at a much higher rate than any other defect. This effect leads to the dark contrast of the APBs in SEM versus other features in the sample surface. Thus, an accurate count of the density of APBs that intersect the GaAs surface can be determined.

Sources of APBs

There is an apparent effect from the presence of oxygen and/or carbon contamination on the Si substrate prior to growth and the density of APBs in the grown GaAs layer. It is intuitive that surface contamination on the substrate can degrade overall sample quality, as has been demonstrated in previous studies (2, 7-10). The irregularity introduced by surface impurities becomes a source of growth defects in the material, e.g. stacking faults. It follows then that oxide or carbide particles, agglomerated from residual oxygen or carbon on the Si surface, can also promote the formation of APBs due to the disruption in ordering of the epitaxial GaAs layer. This is in addition to the inherent effect of single steps that are present on the substrate.

The source of oxygen contamination on the Si surface is likely from the incomplete removal of the native oxide due to variations in the pre-clean procedure. However, the interfacial oxygen doses only corresponded to a fraction of a monolayer. Carbon on the Si surface likely stems from incomplete desorption of precursor reaction products or desorption from the MOCVD chamber walls as the substrate temperature is increased to the growth temperature. The former could also be a side effect of interaction with residual oxygen contamination from the incomplete removal of the native oxide. The interfacial carbon dose for the samples was on the order of a monolayer of coverage and was about two orders of magnitude greater than the corresponding oxygen doses. However, it is not clear at this point whether it is an oxide or carbide impurity that is promoting the formation of APBs, since only the native oxide pre-clean was varied and both the oxygen and carbon interfacial doses increase with APB density.

More analysis is needed to determine the nature of the correlation between substrate surface contamination and APB density, and whether it is residual oxygen or carbon forming amorphous particles that is contributing to the increased presence of APBs. There is an implication of a threshold effect from either the oxygen or carbon contamination that causes a significant increase in APB density and change in behavior. Reducing the presence of these species below a certain level, and thus reducing the APB density, will allow for the complete suppression of APBs in GaAs directly grown on Si without high-temperature pre-growth treatments at lower layer thicknesses. This effect arises from the natural tendency of APBs to self-annihilate in the bulk to reduce the free energy of the system. The greater the density of APBs, the more difficult it is to have all APBs completely self-annihilate within a given layer thickness.

Conclusions

A quantitative analysis of the effect of oxygen and carbon interfacial contamination on APB density in an epitaxial GaAs layer grown on Si(100) was performed in this study. A combination of SIMS analysis and an APB-sensitive chemical etch was used to investigate the relationship after varying the pre-clean of the wafer prior to GaAs growth. It was found that for an increase in interfacial oxygen dose from $7.3x10^{11}$ to $4.0x10^{12}$ atoms/cm^2 and increase in interfacial carbon dose from $1.9x10^{14}$ to $1.7x10^{15}$ atoms/cm^2, the APB density significantly increases from 0.14 to 3.2 μm^{-1}. The increased APB density causes a switch in behavior from tendency towards self-contained domains to extended lines of APBs. It is believed that residual oxygen or carbon contamination left by the pre-clean of the Si wafer leads to the formation of amorphous oxide or carbide particles on the surface. These particles in turn disrupt the ordering of the epitaxial layer, inducing the formation of both stacking faults and APBs. It is difficult to fully prevent the formation of APBs without a high-temperature treatment of the Si substrate to promote the presence of double-steps. The formation of additional APBs from interfacial impurities hinders the likelihood of complete APB self-annihilation within the bulk GaAs layer. This is believed to be the first quantitative correlation between the oxygen/carbon contamination and APB density, of particular relevance to reduced thermal budget semiconductor processing.

Acknowledgments

This work is funded through a research grant by Applied Materials. The authors acknowledge the Major Analytical Instrumentation Center at the University of Florida for the use of the focused ion beam and transmission electron microscopy facilities.

References

1. J. A. del Alamo, *Nature*, **479**, 317–323 (2011).
2. S. F. Fang et al., *J. Appl. Phys.*, **68**, R31–R58 (1990).
3. I. Németh, B. Kunert, W. Stolz, and K. Volz, *J. Cryst. Growth*, **310**, 1595–1601 (2008).
4. M. Grundmann, et al., *J. Vac. Sci. Technol. B*, **9**, 2158 (1991).
5. T. Sakamoto and G. Hashiguchi, *Jpn. J. Appl. Phys.*, **25**, L78 (1986).
6. R. J. Hamers, R. M. Tromp, and J. E. Demuth, *Phys. Rev. B*, **34**, 5343–5357 (1986).
7. Z. Liliental-Weber, E. R. Weber, L. Parechanian-Allen, and J. Washburn, *Ultramicroscopy*, **26**, 59–63 (1988).
8. A. E. Blakeslee, M. M. Al-Jassim, J. M. Olson, K. M. Jones, and S. M. Vernon, *MRS Symp. Proc.*, vol. **116**, 313 (1988).
9. Z. Liliental-Weber, *MRS Symp. Proc.*, vol. **148**, 205 (1989).
10. Z. Liliental-Weber and R. P. Mariella, *MRS Symp. Proc.*, vol. **148**, 241 (1989).
11. M. Akiyama, Y. Kawarada, T. Ueda, S. Nishi, and K. Kaminishi, *J. Cryst. Growth*, **77**, 490–497 (1986).
12. D. K. Biegelsen, F. A. Ponce, A. J. Smith, and J. C. Tramontana, *J. Appl. Phys.*, **61**, 1856–1859 (1987).
13. R. Yang et al., *J. Vac. Sci. Technol. B*, **28**, 56–61 (2010).
14. S. N. G. Chu, S. Nakahara, S. J. Pearton, T. Boone, and S. M. Vernon, *J. Appl. Phys.*, **64**, 2981 (1988).
15. A. Georgakilas et al., *J. Mater. Res.*, **8**, 1908–1921 (1993).
16. Y. Chriqui et al., *J. Cryst. Growth*, **265**, 53–59 (2004).
17. Rasband, W.S., ImageJ, U. S. National Institutes of Health, Bethesda, Maryland, USA, http://imagej.nih.gov/ij/, 1997-2014.